The application of thermal analysis to the study of epoxy-clay nanocomposites

John M Hutchinson

Departament de Màquines i Motors Tèrmics, ETSEIAT, Universitat Politècnica de Catalunya, 08222 Terrassa, Spain

hutchinson@mmt.upc.edu

Tel: +34 93 739 8123

Fax: +34 93 739 8101

Abstract

The development of polymer layered silicate (PLS) nanocomposites goes back over 20 years now, and yet they still have not achieved their full potential. A principal reason for this is the difficulty of obtaining a truly exfoliated nanostructure. The fabrication procedure for such PLS nanocomposites based upon epoxy resin includes several stages, including dispersion of the clay in the resin, intercalation of the resin into the clay galleries, and finally curing of the nanocomposite system. Many attempts have been made to improve the degree of exfoliation in the final nanostructure by modifying the procedures involved in these fabrication stages, and the usual approach is to examine the nanostructure, by techniques such as Small Angle X-Ray Scattering (SAXS) and Transmission Electron Microscopy (TEM), as a function of the fabrication procedure. We show here, however, that thermal analytical techniques, and in particular Differential Scanning Calorimetry (DSC), can complement the techniques of SAXS and TEM in the search for ways in which to achieve improved degrees of exfoliation in PLS nanocomposites based upon epoxy resin.

Keywords

Differential scanning calorimetry (DSC); nanocomposites; polymer layered silicate (PLS); exfoliation; epoxy resin

Introduction

The development of polymer layered silicate (PLS) nanocomposites goes back over 20 years now, to the pioneering work of the Toyota group on nylon-6 nanocomposites [1-4], in which it was found that major improvements in the physical and mechanical properties of these systems could be achieved with clay contents as low as 2 wt%. This would represent a significant advance over conventional composites, particularly for lightweight structural applications, since the same degree of reinforcement can be achieved with much lower filler loadings. However, the question of whether or not these PLS nanocomposites have yet realised their full potential in respect of applications in engineering is still open to doubt. Some authors claim, for example, that "Epoxy clay nanocomposites are finding vast applications in various industries like aerospace, defense, automobile, etc." [5]. On the other hand, others [6] maintain that "Nanocomposite materials hold the *potential* to redefine the field of traditional composite materials both in terms of performance and *potential* applications" and that "There is little doubt that polymer nanocomposites have tremendous market *potential* both as replacements for current composites and in the creation of new markets through their outstanding properties." This difference of opinion can be associated with the different possible nanostructures that may exist in the final nanocomposite: phase separated, intercalated or exfoliated [7].

It is generally believed that these PLS nanocomposites must attain an exfoliated nanostructure in order to achieve their optimum properties, and in particular to optimise their mechanical properties [7-10]. Despite considerable effort in this task, it has so far proved a difficult goal to reach. According to Liu [11], for example, "much is still unknown concerning the relationships between materials, synthesis, structure and properties of epoxy-clay nanocomposites, especially for structural epoxy resins" and "it is extremely difficult to synthesize completely exfoliated nanocomposites." This author goes on to state that in "TEM images of epoxy-clay nanocomposites in almost all published papers, few exfoliated platelets of clay are observed. As a result, the biggest challenge is how to exfoliate platelets of clay in epoxy resins." This challenge is addressed in the present paper.

The procedures for fabricating the PLS nanocomposites differ according to whether the matrix material is a thermoplastic or a thermoset, and so must be considered separately. In this paper, PLS nanocomposites based upon epoxy resins are considered, and the route towards improved exfoliation is discussed. In particular, the contribution of thermal analytical techniques towards a better understanding of the complete process of nanostructure development in these materials is discussed, and it is shown how such techniques, and in particular Differential Scanning Calorimetry (DSC), can complement the techniques of Small Angle X-Ray Scattering (SAXS) and Transmission Electron Microscopy (TEM) in the search for ways in which to achieve improved degrees of exfoliation in PLS nanocomposites based upon epoxy resin.

PLS fabrication procedure

Dispersion of clay in epoxy resin, and intercalation of resin into clay galleries

For epoxy-based PLS nanocomposites, the fabrication procedure begins with the mixture of the organically modified clay with the epoxy resin. This part of the fabrication procedure is important in respect of the quality of the dispersion of the clay in the epoxy resin, which can depend on a number of factors, including the clay type, the clay loading and the mixing method. The last of these factors may involve, for example, simple mechanical mixing or the so-called slurry method [12-17], in which the clay is first dispersed in a solvent, often acetone, before the resin is added and mixed mechanically, and then finally eliminating the solvent. As an illustration of the different degrees of dispersion that can be achieved by these two methods, we compare a mixture of 5 wt% of organically modified (octadecylammonium) montmorillonite (MMT), Nanomer I.30E (Nanocor Inc.), in diglycidyl ether of bisphenol-A (DGEBA) epoxy resin, Epon 828 (Shell Chemicals), which has an epoxide equivalent weight in the range 185 to 192 g equiv^{-1}, a density of 1.16 g cm^{-3}, and a viscosity in the range 11,000 to 15,000 mPa.s at 25 °C. When the clay and resin were mixed by mechanical stirring at 75 °C for a period of 20 hours, the quality of the dispersion was rather poor, as shown by the optical micrograph in Fig. 1(a). Here it can be seen that, although the majority of the clay agglomerations are of the order of 20 μm or less in size, there are some agglomerations which are much larger, of the order of 50 or 60 μm in size. This is not suitable for subsequently achieving an exfoliated nanostructure in the cured nanocomposite, as the large agglomerations inhibit the intercalation of the epoxy resin into the clay galleries. The slurry dispersion method, on the other hand, results in a much better dispersion for the same clay content in the same epoxy resin, as shown in the optical micrograph in Fig. 1(b).

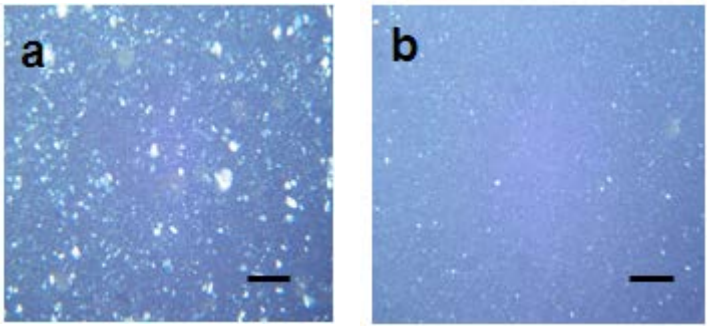

Fig. 1 Transmission optical micrographs, using polarised light, showing the dispersion of 5 wt% MMT in DGEBA epoxy resin: (a) simple mechanical mixing; (b) slurry method, using acetone as solvent. Scale bar is 125 μm

During this mixing and dispersion process, the resin penetrates into the clay galleries and expands the clay layer separation (*d*-spacing) in a process known as intercalation. This effect is conventionally measured by SAXS, and the *d*-spacing is found to increase

from 2.1 nm for the organically modified MMT alone to about 3.5-3.9 nm when the epoxy has intercalated into the clay galleries. This intercalated spacing is essentially independent of the clay loading and of the mixing method, be it hand mixing, mechanical mixing, high shear mixing or solvent mixing [18].

But there is also information that can be gained about the intercalation process by thermal analytical techniques, such as DSC, particularly with respect to the mobility of the resin within the clay galleries. First, the glass transition temperature, T_g, of the epoxy resin alone and of epoxy-clay mixtures with 10 wt% MMT and prepared by different techniques (hand mixing, mechanical stirring, high shear mixing, slurry method using acetone) has been determined by scanning in the DSC from -70 °C to 25 °C at 10 °C min^{-1}, using a Mettler Toledo DSC822 with a 50 mL min^{-1} flow of dry nitrogen. The results are shown in Fig. 2. The scale bar gives the specific heat flow referred to the mass of epoxy resin in each sample; it can be seen that all these curves superpose within experimental error, and there are unique values for the increment in the specific heat capacity, $\Delta c_p = 0.508 \pm 0.006$ J g^{-1} K^{-1}, and for $T_g = -14.0 \pm 0.4$ °C. The implication of this is that the epoxy resin has the same molecular mobility whether it is within the nanometre-sized clay galleries or in the bulk.

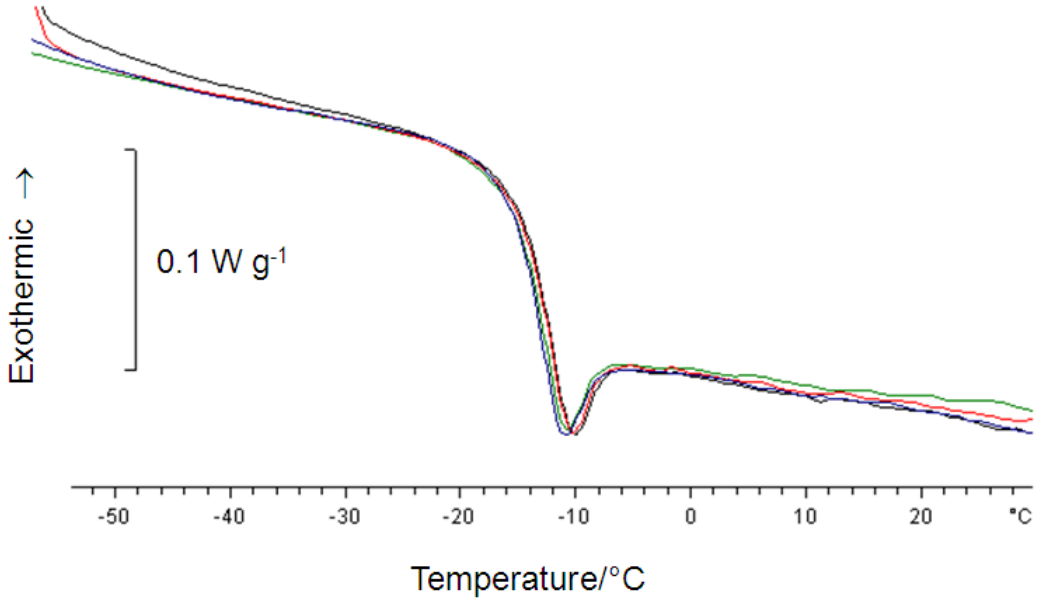

Fig. 2 DSC heating scans at 10 °C min^{-1} for: epoxy resin (green); hand mix (blue); mechanical mix (red); high shear mix (black)

This is further confirmed by performing intrinsic cycles within the glass transition interval for each of these samples: cooling at various rates through the transition region followed by immediately reheating at 10 °C min^{-1} to again reach equilibrium above the glass transition. From such cycles the dependence of the fictive temperature on cooling rate is obtained, and hence the apparent activation for enthalpy relaxation can be found [19-22]. These intrinsic cycles are almost identical for the epoxy resin alone and for the three epoxy-clay samples with 10 wt% MMT prepared by different methods, the reduced apparent activation energy being $\Delta h^*/R = 70 \pm 10$ kK for all these samples.

The observation of a single glass transition with unique values for T_g, Δc_p and $\Delta h^*/R$ implies that the intercalated and bulk epoxy resin have the same molecular mobility. Dielectric analysis (DEA) on the same samples also leads to the same conclusion, as indicated by the results shown in Fig. 3 for the frequency dependence of the peak in tan δ for the α-relaxation of the sample with 10 wt% MMT, mechanically mixed. A single peak is observed, in which the non-linear dependence of ln(frequency) on the reciprocal peak temperature can be fit with a Vogel-Fulcher-Tammann (VFT) equation. If this VFT curve is extrapolated to a frequency of 0.01 Hz, corresponding to the equivalent timescale of 100 s for a DSC measurement, a glass transition temperature of -15 °C is found, and the slope of the VFT curve at this temperature gives the same value of 70 kK for the reduced apparent activation energy as was obtained by DSC.

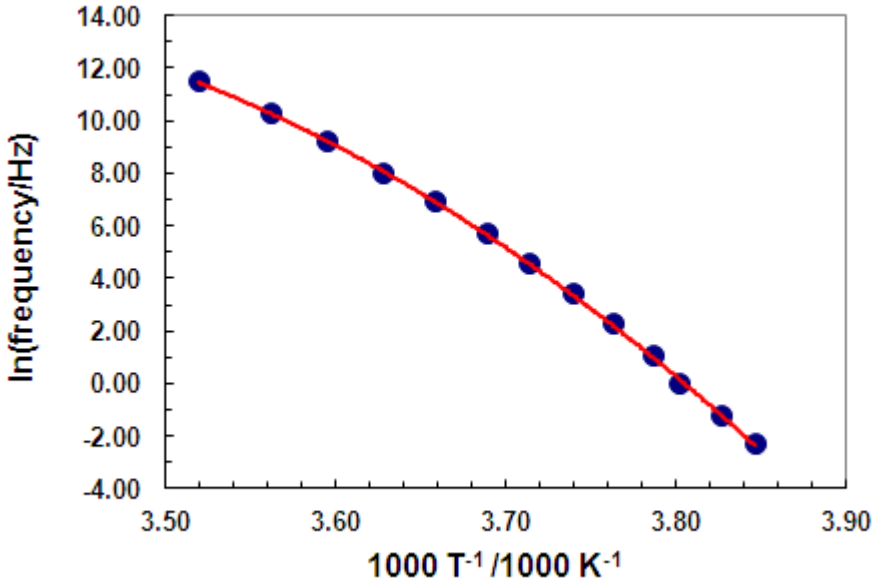

Fig. 3 Relationship between ln(frequency) and reciprocal peak temperature for the α-relaxation of the epoxy-clay mixture with 10 wt% MMT obtained by dielectric analysis. The curve through the experimental points corresponds to the VFT equation

On the other hand, it is possible under some circumstances to distinguish between the molecular mobility of the epoxy resin in the bulk and within the clay galleries. An epoxy-clay mixture with a very high clay content (25 wt%, deliberately used in order to emphasise the effect), prepared by the solvent method using acetone, was scanned in the DSC at 10 °C min^{-1} from -70 °C to 25 °C in order to determine its glass transition temperature, but before the elimination of the solvent. The same sample, without removing it from the DSC furnace, was then repeatedly cooled back to -70 °C and scanned again under the same conditions. The results are shown in Fig. 4(a).

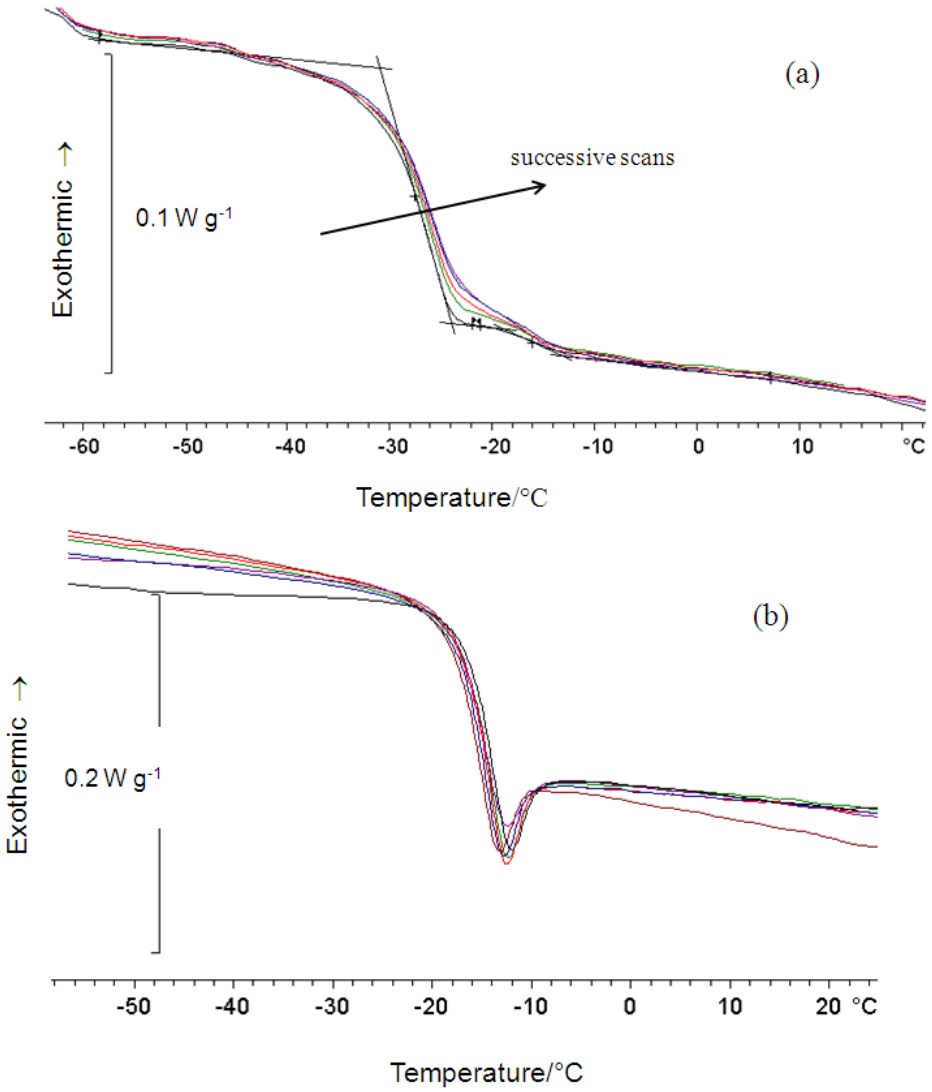

Fig. 4 (a) Successive DSC scans at 10 °C min^{-1} for a solvent-prepared epoxy-clay mixture with 25 wt% MMT. **(b)** DSC scans at 10 °C min^{-1} after complete elimination of the solvent for samples with different wt% MMT: 5 (green), 10 (red), 15 (dark blue), 20 (purple), 25 (brown)

In the first (leftmost) scan, two glass transitions are clearly seen: the lower one at about -28 °C and with Δc_p = 0.482 J g^{-1} K^{-1} corresponds to the bulk extra-gallery epoxy resin plasticised by the acetone, whereas the higher one at about -16 °C and with Δc_p = 0.048 J g^{-1} K^{-1} corresponds to the intercalated epoxy resin within the clay galleries which has hardly been plasticised by the solvent. With each successive scan some solvent is eliminated, resulting in a gradual shift of the lower glass transition towards higher temperatures. As more and more solvent is eliminated, the two glass transition temperatures merge, and eventually, after complete elimination of the solvent, the DSC scan for this epoxy-clay mixture with 25 wt% MMT again resembles that of the epoxy alone, as shown in Fig. 4(b). In fact, included in Fig. 4(b) are the results for solvent-prepared epoxy-clay mixtures with clay contents of 5, 10, 15, 20 and 25 wt% MMT, for all of which the same return to the behaviour of the epoxy resin alone is observed once the acetone has been completely removed.

The relative magnitudes of the Δc_p steps for the extra- and intra-gallery regions in Fig. 4(a) allow an estimate to be made of the proportion of resin that is within the clay galleries. This analysis has been made previously [18], and from a comparison with what would be expected from the *d*-spacing determined by SAXS it was concluded that the epoxy resin does not penetrate fully into the clay galleries. Indeed, it was estimated that it penetrates only to about one third of the distance towards the centre of the clay particles, which would have important consequences for the subsequent curing and exfoliation process. In fact, TEM micrographs of cured nanocomposites often show a nanostructure in which clay layers remain in close register in one region while being well separated at another extreme. This is illustrated in Fig. 5.

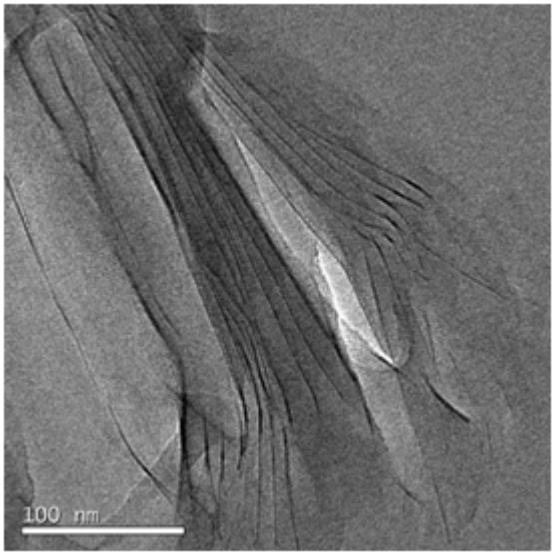

Fig. 5 TEM micrograph of a tri-functional epoxy nanocomposite with 5 wt% MMT cured with diaminodiphenyl sulphone

Curing of resin-clay mixtures

Following intercalation of the resin into the clay galleries, the subsequent and final step is to add the curing agent and effect the cross-linking reaction so as to achieve a fully cured nanocomposite. It is during this stage of the overall fabrication procedure that the transformation to an exfoliated nanostructure should take place. However, a fully exfoliated nanostructure is difficult to achieve, and furthermore the mechanisms involved in the exfoliation process are not well understood. The degree to which exfoliation has been achieved can be assessed to a certain extent by SAXS, which indicates whether or not there remain significant numbers of clay layers in register, for which a scattering peak corresponding to their *d*-spacing will appear. This, however, has the limitation that *d*-spacings greater than about 8 nm cannot be detected because of the background scattering. Accordingly, it is common practice in addition to examine the nanostructure of the cured nanocomposite by TEM.

Besides these nanostructural characterisation techniques of SAXS and TEM, however, there is much useful information to be gained about the exfoliation process by thermal analysis, and in particular by DSC. First, a homopolymerisation reaction that takes place in the resin as a consequence of the catalytic action of the organically modified clay is an important factor in the nanostructure development, and provides one route towards an improved degree of exfoliation, known as pre-conditioning. Second, the overall reaction that occurs in the nanocomposite system consisting of epoxy resin, clay and curing agent is very complicated, and can be deconvoluted into several different reactions, which may or may not occur simultaneously. Third, these various reactions may take place either within the clay galleries or outside the clay galleries. All of these aspects contribute to the nature of the final nanostructure in the cured nanocomposite. In this section the use of DSC in this respect is illustrated by means of a number of examples.

DGEBA-clay system cured with Jeffamine

DGEBA epoxy is mixed with 10 wt% organically modified MMT and then cured non-isothermally with a stoichiometric amount of polyoxypropylene diamine (Jeffamine D-230, Huntsman). The exothermic reactions observed by DSC for different rates of heating are shown in Fig. 6. A noticeable feature of these cure curves is the appearance of a shoulder on the high temperature flank, which can be seen very clearly by comparison with the fit of an autocatalytic model to these curves:

$$f(\alpha) = \alpha^m (1-\alpha^n) \qquad (1)$$

where α is the degree of cure and m and n are the kinetic exponents of the reaction [23]. This theoretical fit is indicated by the dash-dotted lines in Fig. 6, and shows that the departure from the theoretical model occurs at a degree of cure of about 65%. This is indicative of a further reaction that is occurring in addition to the bulk cross-linking reaction of the epoxy resin with the diamine, this further reaction being attributed to the homopolymerisation of the epoxy resin within the clay galleries, catalysed by the onium ion of the organically modified clay [24, 25].

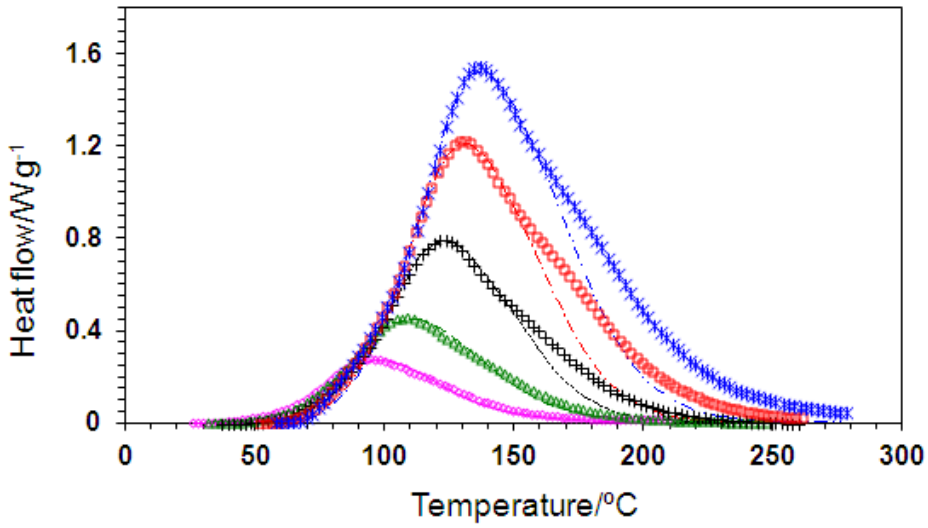

Fig. 6 DSC cure curves for DGEBA epoxy with 10 wt% MMT cured with Jeffamine at the following rates, increasing from bottom to top: 2.5 °C min^{-1} (pink); 5 °C min^{-1} (green); 10 °C min^{-1} (black); 15 °C min^{-1} (red); 20 °C min^{-1} (blue). Dash-dotted lines show fit of autocatalytic model

This is confirmed by comparing the cure of these nanocomposite systems with different clay contents, as shown in Fig. 7. For the epoxy-Jeffamine system without any clay, the autocatalytic model provides an excellent fit to the cure curve. With increasing clay content, however, an additional reaction occurs, appearing as a shoulder which increases in magnitude with increasing clay content, and for which the departure from the theoretical fit occurs at about 65% degree of cure.

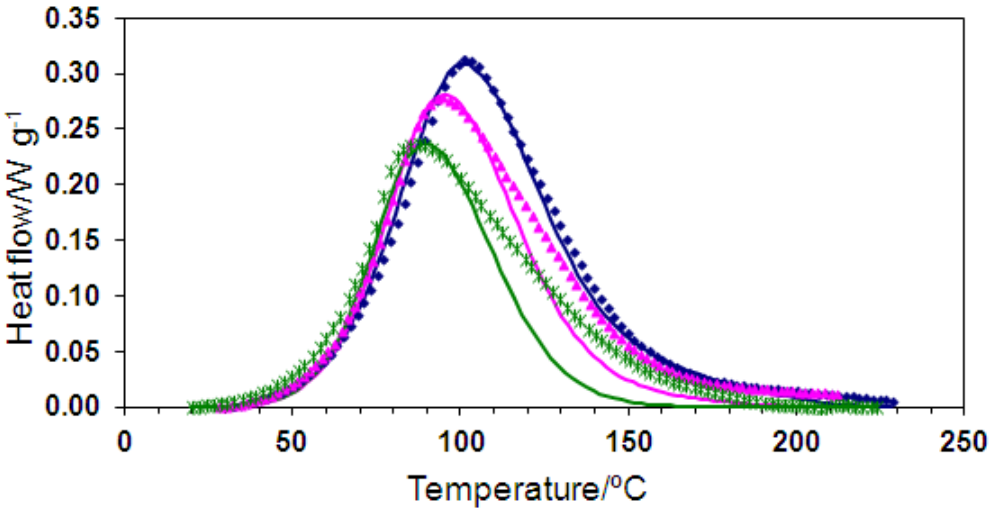

Fig. 7 DSC cure curves for DGEBA epoxy-clay mixtures cured with Jeffamine, for the following clay contents: no MMT (purple); 10 wt% MMT (pink); 20 wt% MMT (green). Full lines show fit of autocatalytic model

The important aspect of the appearance of this shoulder in the reaction kinetics is that it occurs *after* the main peak. If there is a significant amount of intra-gallery reaction occurring after 65% of the bulk cross-linking reaction has already taken place, this means that this intra-gallery reaction will not result in exfoliation of the clay layers because they are embedded in an already rather rigid matrix. The same conclusion can be reached from an analysis of the isothermal curing kinetics of the same nanocomposite system, using the procedure devised by Malek [26]. According to this procedure, the equation for the dependence of the heat flow, ϕ, on the degree of cure can be written in the form:

$$\ln(\phi e^{x}) = \ln(A\,\Delta H) + n\,\ln[\alpha^{m/n}\,(1-\alpha)] \qquad (2)$$

where $x = E/RT$ is a dimensionless function of the activation energy E, A is the pre-exponential factor, and ΔH is the total heat of reaction. Thus a plot of $\ln(\phi e^{x})$ as a function of $\ln[\alpha^{m/n}(1-\alpha)]$ should yield a straight line with a slope equal to the kinetic exponent n. When this approach is applied to the analysis of the isothermal cure at 70 °C of a DGEBA-Jeffamine nanocomposite system with 20 wt% MMT, the results obtained are shown in Fig. 8. It can clearly be seen that there are two distinct regions, with two different slopes and hence two different values for the kinetic exponent: n = 1.8 in the initial stages of the cure, and n = 1.4 in the final stages, with the cross-over occurring at a degree of cure of between 0.6 and 0.7, in agreement with the observations from the non-isothermal cure kinetics.

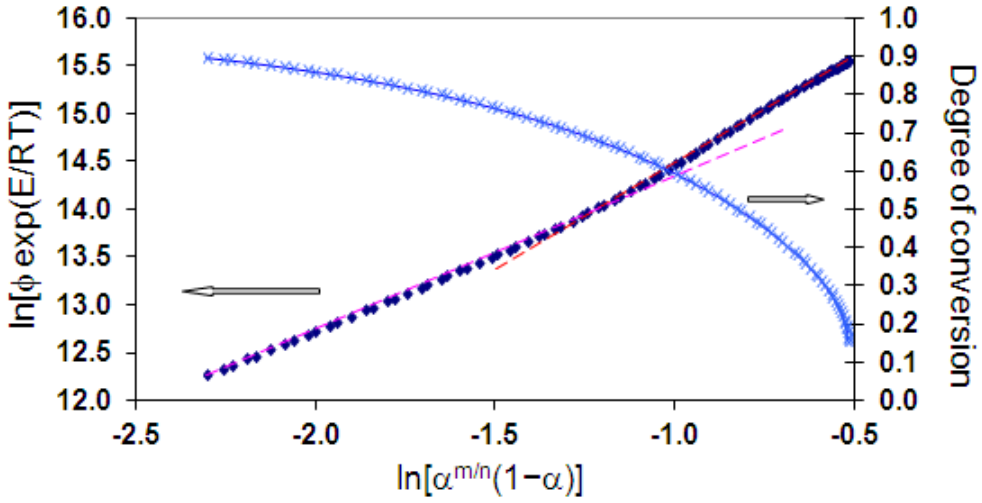

Fig. 8 Kinetic analysis of the isothermal cure of DGEBA-Jeffamine system with 20 wt% MMT at 70 °C. Blue crosses refer to degree of conversion on right-hand axis; filled symbols refer to the left-hand axis; dashed lines show linear fits to the initial and final stages of the cure. Note that in this figure the reaction proceeds from right to left

It can be concluded from this kinetic analysis of both the isothermal and non-isothermal cure of these nanocomposite systems based on DGEBA epoxy resin cured with Jeffamine that there are two reactions occurring, and that the change from one to the other occurs at a degree of conversion of approximately 65%. The two reactions are identified as, first, the bulk cross-linking reaction of the epoxy and Jeffamine and, second, an intra-gallery homopolymerisation reaction of the epoxy resin. Since it is this intra-gallery reaction which should lead to exfoliation, and since this reaction evidently occurs too late, after a substantial part of the surrounding bulk resin has cured, it is to be anticipated that this nanocomposite system will not be well exfoliated. This is confirmed by nanostructural characterisation techniques. SAXS displays a sharp scattering peak at an angle corresponding to a *d*-spacing of only 1.4 nm, which is less than that of the intercalated clay (3.5-3.9 nm), and even less than that of the clay before

intercalation of the epoxy resin (2.1 nm). This is a consequence of the fact that the bulk resin cures first: this cure is accompanied by a contraction in the volume, which compresses the clay agglomerations in which the intra-gallery homopolymerisation reaction has yet to occur, and which cannot lead to exfoliation because of the constraint imposed by the rigid matrix. The TEM micrographs of the cured nanocomposite, such as that illustrated in Fig. 9, show a considerable number of clay layers in close register, and very little evidence of exfoliation. This is a direct consequence of the relative rates of intra- and extra-gallery reactions in these nanocomposite systems, which are clearly identified by thermal analysis.

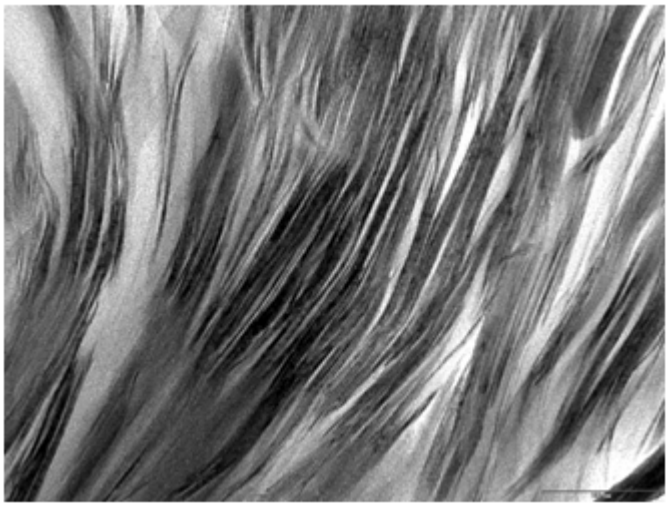

Fig. 9 TEM micrograph at 250,000× magnification for DGEBA-clay system with 10 wt% MMT, mixed mechanically and cured with Jeffamine. Scale bar is 100 nm

Homopolymerisation of DGEBA-clay system

In the DGEBA-clay system cured with Jeffamine described above, the reaction which should lead to exfoliation of the clay layers is the intra-gallery homopolymerisation reaction, but it occurs too late, after the main cross-linking reaction. It might be argued that if this intra-gallery reaction could be promoted to occur earlier, then much better exfoliation would be observed. One way in which this homopolymerisation reaction can be promoted is by pre-conditioning the resin-clay mixture before adding the curing agent and effecting the curing reaction to produce the fully cured nanocomposite. This pre-conditioning procedure was first noted by Benson Tolle and Anderson [27] to be beneficial for the exfoliation process, and involves storage of the resin-clay mixture at a controlled temperature. During this storage time, and following either an activated monomer or activated chain end mechanism in the cationic homopolymerisation process, depending on the storage temperature, both the T_g and the epoxy equivalent increase, the relationship between the two being essentially linear [28]. The observation that in the pre-conditioned samples there is only a single glass transition temperature implies that the homopolymerisation process is occurring in both the intra-gallery and

extra-gallery regions simultaneously, and hence pre-conditioning does not satisfy the requirement identified above that the intra-gallery reaction should occur first. Nevertheless, pre-conditioning is still beneficial for exfoliation because it leads to a significant improvement in the dispersion of the clay in the resin without any significant change in the *d*-spacing of the intercalated clay. This is illustrated in Fig. 10 for the same 5 wt% mixture of MMT in DGEBA for which the dispersion after simple mixing and the slurry method was shown earlier in Fig. 1. Comparing this micrograph with those shown in Fig. 1 it can be seen that a remarkable improvement in the dispersion results from the pre-conditioning process, which promotes the access of the epoxy to the clay galleries and hence leads to an improvement in the degree of exfoliation in the cured nanocomposite. This, however, can be considered to be a complementary procedure for improving the exfoliation, in addition to that based upon accelerating the intra-gallery reaction. In respect of the latter procedure, an alternative would be to investigate the use of a different cross-linking agent from the polyoxypropylene diamine, Jeffamine, used above.

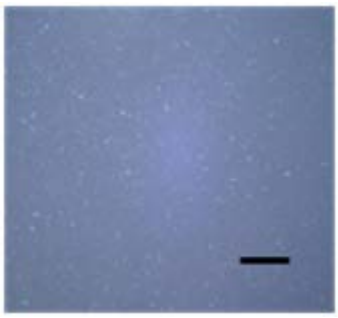

Fig. 10 Transmission optical micrograph using polarised light, showing the dispersion of 5 wt% MMT in DGEBA epoxy resin after pre-conditioning for 3 years at room temperature. Scale bar is 125 μm

DGEBA-clay system cured with a hyperbranched polymer (HBP)

As an alternative to Jeffamine as a curing agent, a commercial hyperbranched polyethyleneimine, Lupasol PR8515 (BASF), was used with the same DGEBA epoxy resin as earlier. The structure of Lupasol PR8515 is shown in Fig. 11.

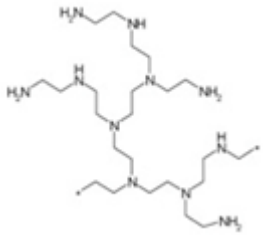

Fig. 11 Structure of hyperbranched polyethyleneimine, Lupasol PR8515

Stoichiometric amounts of the hyperbranched polymer (HBP) were added to the epoxy-clay mixtures containing different weight fractions of clay (2, 5 and 10 wt%), previously prepared by mechanical mixing followed by an ultrasonic bath and sonication [29, 30]. These samples were then scanned in the DSC at 20 °C min^{-1}, and the resulting exothermic reactions are shown in Fig. 12. The usual acceleration of the reaction on the addition of clay is observed, indicated by the arrow, though the curves for the system without clay and that for 2 wt% clay content are almost superposed. However, the more important aspect of these curves in the present context is that they appear symmetrical: there is no shoulder on the high temperature flank as there was for the same epoxy-clay mixtures cured with Jeffamine, for which the equivalent cure curves were shown earlier in Figs. 6 and 7. We know that an intra-gallery reaction must still be occurring in this system, for example because it is found that the T_g of these cured nanocomposites decreases with increasing clay content, as a consequence of the homopolymerisation that takes place within the clay galleries [29, 30]. The reason for the disappearance of the shoulder, therefore, must be that the cure kinetics with this HBP are such that the intra-gallery reaction is now occurring faster in relation to the extra-gallery reaction, such that the intra-gallery reaction is now hidden underneath the main cross-linking peak.

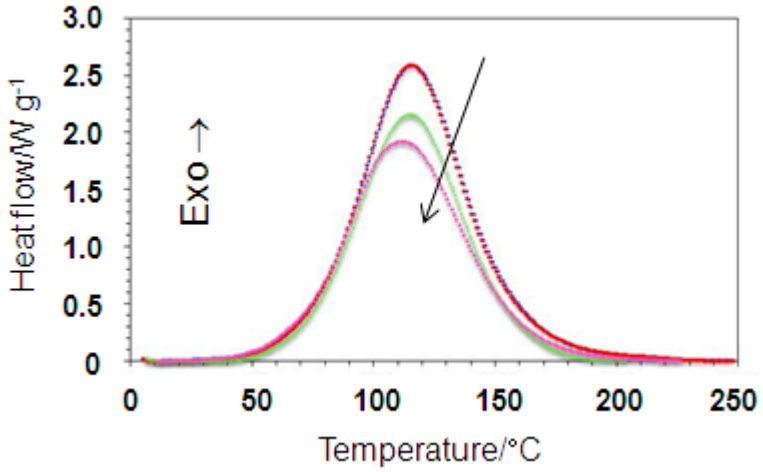

Fig. 12 DSC cure curves for DGEBA epoxy-clay mixtures cured at 20 °C min^{-1} with Lupasol HBP, for the following clay contents: no MMT (blue); 2 wt% MMT (red); 5 wt% MMT (green); 10 wt% MMT (pink). Arrow shows direction of increasing clay content

The implication of this would be that these cured nanocomposites should be better exfoliated than those prepared by curing with Jeffamine. This is indeed observed when these samples are samples are studied by SAXS and TEM. The SAXS diffractograms do not show any intense scattering peaks, such as those seen in the same system cured with Jeffamine at scattering angles corresponding to *d*-spacings as low as 1.4 nm, which is suggestive of an exfoliated nanostructure but which requires confirmation by TEM. A

typical TEM image for one of these nanocomposites with 2 wt% clay and cured with the HBP is shown in Fig. 13(a), and should be compared with that of Fig. 13(b) for the same epoxy-clay mixture with 2 wt% clay cured with Jeffamine. The difference between the two nanostructures is remarkable. Even though the nanostructure in Fig. 13(a) is clearly not fully exfoliated, the separation of the clay layers is greater for the HBP-cured system and there is much less layer stacking. These nanostructures therefore support the conclusion reached form a consideration of the thermal analysis data, namely that the use of Lupasol HBP as a curing agent for these layered silicate nanocomposites leads to a much greater degree of exfoliation in comparison with that achieved using Jeffamine as a curing agent.

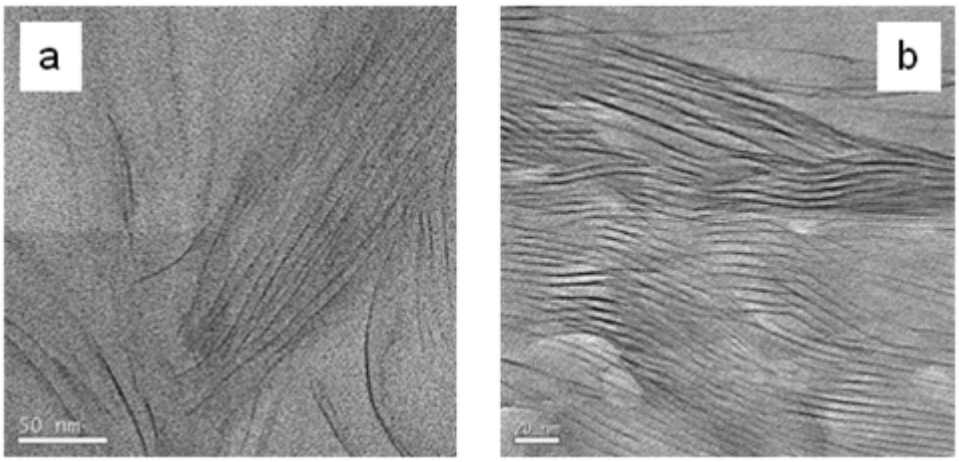

Fig. 13 TEM micrographs for DGEBA-clay system with 2 wt% MMT: (a) cured with polyethyleneimine HBP; (b) cured with Jeffamine. Scale bars are 50 nm (a) and 20 nm (b)

TGAP-clay system cured with diaminodiphenyl sulphone (DDS)

An alternative approach to achieving improved exfoliation in these PLS nanocomposites is to use a different type of epoxy resin. Here, instead of the bifunctional DGEBA epoxy, we make use of a tri-functional resin, triglycidyl p-amino phenol, TGAP (Araldite MY0510, Huntsman Advanced Materials), cured with 4,4-diamino diphenyl sulphone, DDS (Aradur 976-1, Aldrich). Mixtures of TGAP epoxy resin with 2, 5 or 10 wt% MMT were first prepared by mechanical mixing and then the required amount of curing agent, to give a slight excess of epoxy (1:0.85 molar, TGAP:DDS) with respect to the stoichiometric ratio [31-33], was added and mixed at 80 °C on a hot-plate for 5-7 minutes. The cure kinetics were then monitored during isothermal DSC experiments at several cure temperatures. Typical results are shown in Fig. 14(a) for the isothermal cure of a 5 wt% MMT nanocomposite at the cure temperatures of 150, 165 and 180 °C.

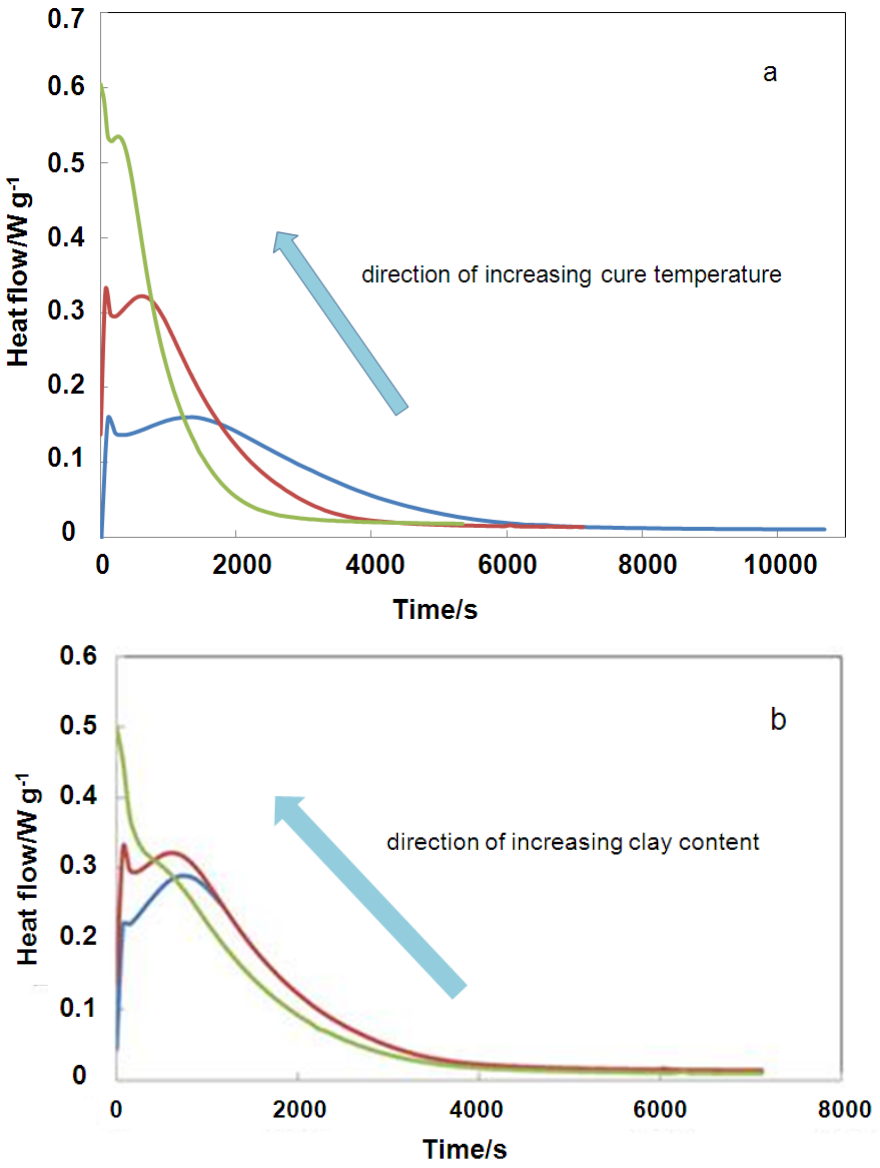

Fig. 14 Isothermal cure curves for TGAP-clay mixtures: (a) with 5 wt% MMT and cured with DDS at 150 °C (blue), 165°C (red) and 180 °C (green); (b) cured at 165 °C with 2 wt% MMT (blue), 5 wt% MMT (red) and 10 wt% MMT (green)

The most important aspect of these cure curves is the appearance of a sharp peak at the very beginning of the cure: this corresponds to an intra-gallery reaction, and is clearly occurring very rapidly and before the cross-linking reaction of the epoxy with the DDS, which gives the subsequent large bell-shaped curve for each of the cure temperatures. There are two reasons for attributing this first sharp peak to an intra-gallery homopolymerisation reaction: first, because with an increase in clay content the peak becomes more pronounced, as shown in Figure 14(b); and second, because in those TGAP epoxy-clay mixtures which have been pre-conditioned before curing with the addition of the DDS, the initial sharp peak does not appear as a consequence of the intra-gallery homopolymerisation reaction having already occurred during the pre-conditioning process [34].

This TGAP-clay system cured with DDS therefore presents a situation in which the intra-gallery reaction occurs *before* the extra-gallery reaction, at least in part, and hence would be expected to result in a better degree of exfoliation. Before examining by SAXS and TEM whether or not this is the case, though, it is pertinent to consider what would be the optimum isothermal cure temperature, which would be the temperature for which the greatest amount of intra-gallery reaction occurs. By deconvoluting the composite peaks, such as those shown in Figs. 14(a) and 14(b), into two separate peaks corresponding to the intra-gallery (first peak) and extra-gallery (second peak) reactions, it is found that the heat of reaction of the first peak increases with increasing cure temperature [34]. Consequently, it would be expected that the greatest degree of exfoliation would be obtained for those nanocomposites cured at 180 °C, and this is indeed found when the nanostructures are examined by TEM. Fig. 15 shows the typical nanostructure obtained when these TGAP-clay samples with 5 wt% MMT are cured isothermally with DDS at (a) 120 °C, (b) 150 °C and (c) 180 °C. For cure at 120°C, it can be seen that there are still regions in which the clay layers are parallel and separated by only about 2 nm, although there are also regions where the layers are much better separated, by 10 nm and more. For cure at 150 °C, the clay layers are now much better separated, even in the regions in which they remain rather parallel, the layer separation here being typically about 8 nm or more, while outside these regions the separation is considerably greater. Finally, for cure at 180 °C, the clay layers are no longer in register, and the nanostructure can be considered to be rather well exfoliated. This nanostructural characterisation is therefore in agreement with the predictions from the analysis of the cure kinetics by DSC.

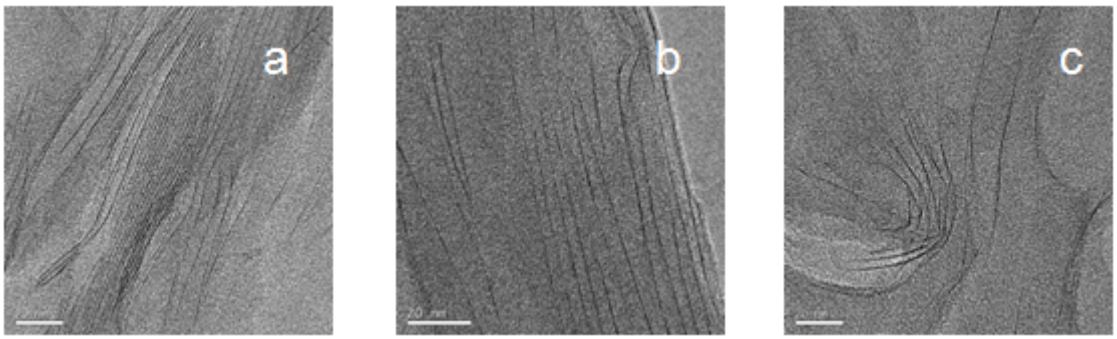

Fig. 15 TEM micrographs for TGAP-clay samples with 5 wt% MMT cured isothermally with DDS at: (a) 120 °C; (b) 150 °C; (c) 180 °C. The scale bar for all micrographs is 20 nm

TGAP-clay system incorporating boron trifluoride initiator

The TGAP-based nanocomposite system is clearly better than the DGEBA-based system in respect of the degree of exfoliation that can be achieved. Nevertheless, although there is a significant amount of intra-gallery homopolymerisation, identified

by the first peak in Fig. 14, which leads to the separation of the clay layers, the complete reaction of the intercalated epoxy resin does not occur before it is inhibited by the bulk cross-linking reaction of the surrounding matrix material. This is evident from the fact that the two peaks in Fig. 14 are superposed rather than being separated on the time scale. In order to maximise the amount of intra-gallery reaction that can take place before the bulk cross-linking reaction, it is necessary somehow to promote the intra-gallery reaction. One way to do this, as discussed above, is to pre-condition the epoxy-clay mixtures before the addition of the curing agent. However, this results in a homopolymerisation reaction not only within the clay galleries but also in the bulk. An alternative procedure is to intercalate an initiator of cationic homopolymerisation into the clay galleries.

The initiator selected was a boron trifluoride monoethylamine (BF_3·MEA) complex, which is known to be an efficient initiator for the homopolymerisation of epoxy resins [35-37]. The BF_3·MEA and MMT were mixed together in various proportions (to give 0.5 wt% and 1.0 wt% for BF_3·MEA, and 2 wt% and 5 wt% for MMT, both with respect to TGAP) using acetone as a solvent, which was subsequently removed. The resulting mixture was ground to a fine powder and dispersed in the epoxy resin by high shear mixing before adding the DDS curing agent by mixing at 80 °C for 5-7 minutes [31, 38]. The SAXS powder diffraction pattern for the MMT+BF_3·MEA shows a marked change in the *d*-spacing of the clay from that of the MMT alone, involving a decrease from 2.1 nm ($2\theta = 4.2°$) to 1.3 nm ($2\theta = 6.8°$), as can be seen in Fig. 16(a). Despite this decrease in the *d*-spacing, however, when the TGAP epoxy intercalates into the clay galleries the *d*-spacing increases dramatically, and reaches a value of 4.4 nm ($2\theta = 2.0°$), significantly larger than the *d*-spacing for the TGAP intercalated into the MMT without the BF_3·MEA complex. It is clear, therefore, that this procedure results in the presence of both BF_3·MEA initiator and TGAP epoxy within the clay galleries before the addition of the curing agent. Nevertheless, it is worth pointing out that the SAXS diffractogram of Fig. 16(b) still shows a very small scattering peak at $2\theta = 6.8°$, corresponding to a *d*-spacing of 1.3 nm, which indicates that the epoxy resin has not fully intercalated, and that there remain some clay layers in very close register. This has implications for the final nanostructure, and will be discussed later by reference to the corresponding TEM images.

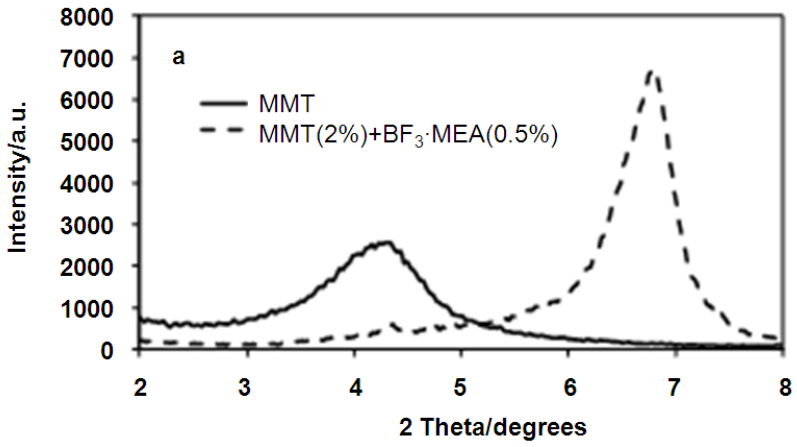

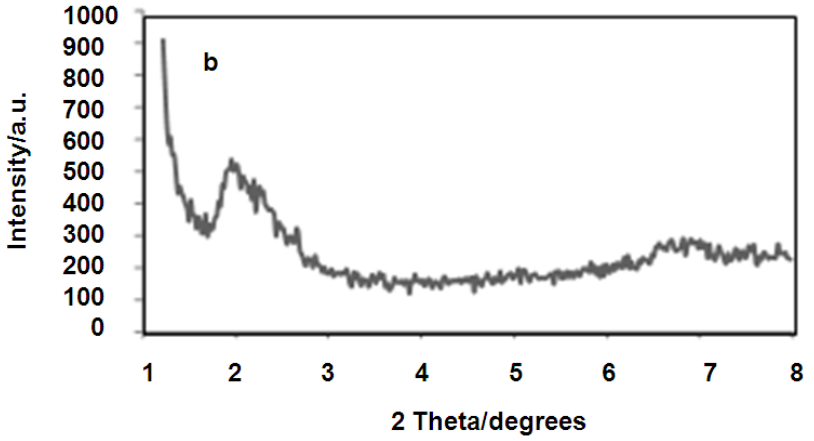

Fig. 16 SAXS diffractograms for: (a) MMT, full line, and MMT modified with BF_3·MEA, dashed line; (b) MMT modified with BF_3·MEA after intercalation of TGAP

This TGAP-MMT-BF_3·MEA-DDS system is now ready for curing, but the curing must be done in two isothermal stages. The first stage is at a temperature of 100 °C or 110 °C, sufficiently high for the homopolymerisation reaction within the clay galleries to be initiated by the BF_3·MEA but not high enough for the extra-gallery cross-linking reaction with the DDS to occur to any significant extent. This stage therefore permits the clay layers to exfoliate as a consequence of the intra-gallery reaction, while not being inhibited by the gradual cure of the surrounding matrix. On the completion of this first stage, the second isothermal stage, at temperatures from 150 °C to 180 °C, results in the cross-linking reaction of the TGAP with the DDS in the bulk regions of the nanocomposite. The temperature range of 100 °C to 110 °C for the first stage cure was identified from a series of isothermal experiments to find the range of temperatures for which the first stage cure was maximised and the second stage cure was minimised.

The cured nanocomposites fabricated in this way, for clay contents of both 2 wt% and 5 wt% and for both contents of BF_3·MEA (0.5 wt% and 1 wt%), show a complete absence of scattering peaks in the low angle region, suggesting that these samples are exfoliated. However, close examination shows that all the samples display a very small scattering peak at a double angle of about 6.8°, corresponding to a *d*-spacing of 1.3 nm and resulting from the small fraction of the BF_3·MEA-modified clay into which the TGAP resin does not intercalate, as noted in respect of Fig. 16(b) [38]. This will also be seen when the TEM micrographs are examined.

Comparison of the TEM micrographs for the samples prepared with and without the BF_3·MEA initiator show that the number and average size of the clay agglomerations dispersed throughout the bulk of the sample are significantly reduced on the incorporation of the BF_3·MEA, as can be seen in the low magnification TEM images in Fig. 17. For the TGAP-clay nanocomposite with 5 wt% MMT cured isothermally at 180

°C, the TEM image in Fig. 17(a) shows that there remain some clay agglomerations in the cured nanocomposite, the largest one here being about 5 μm in size. In contrast, the 5 wt% MMT nanocomposite prepared by first incorporating BF_3·MEA into the clay galleries, shown in Fig. 17(b), has fewer agglomerations, which are also smaller, the largest one shown here being significantly less than 5 μm in size. If one of these latter agglomerations is examined at higher magnification, as shown in Fig. 17(c), it can be seen that there are some clay layers in very close register, with a *d*-spacing of the order of 1.3 nm. This is the separation of the clay layers after the intercalation of the BF_3·MEA, and it was shown earlier by SAXS that a fraction of the clay was not subsequently intercalated by the TGAP epoxy resin, leaving a small peak at $2\theta = 6.8°$ that can be seen in Fig. 16. This is the origin of the very closely packed clay layers in Fig. 17(c).

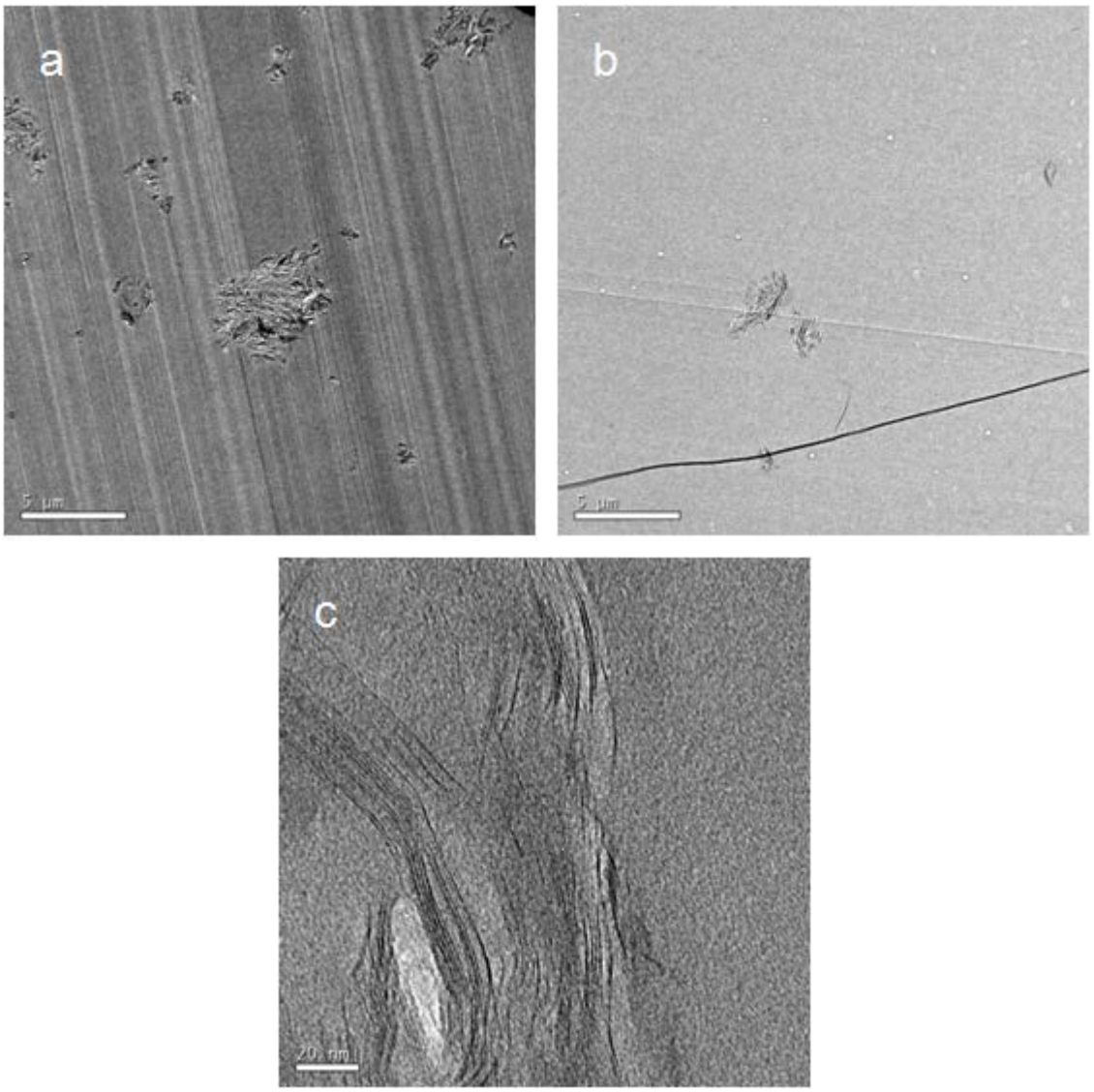

Fig. 17 TEM micrographs of cured nanocomposites: (a) TGAP-MMT(5 wt%), 180 °C, without BF_3·MEA, 800× magnification, scale bar 5 μm; (b) TGAP-MMT(5 wt%), with 1 wt% BF_3·MEA, 800× magnification, scale bar 5 μm; (c) TGAP-MMT(5 wt%), with 1 wt% BF_3·MEA, 120000× magnification, scale bar 20 nm

The nanostructure of the cured TGAP-clay nanocomposites in which BF_3·MEA is first incorporated into the clay galleries is therefore seen to be significantly better than that of the same system without BF_3·MEA. Indeed, the progression of the improvement in the nanostructure, first with the increase of the isothermal cure temperature, then with pre-conditioning, and finally with the use of BF_3·MEA as an initiator, has not only been demonstrated by TEM but has also been anticipated from the analysis of the DSC cure kinetics. Further confirmation of this progressive improvement is also afforded by measurements of the impact strength of the cured nanocomposites, as indicated in Table 1 below [39, 40].

Table 1 Impact energy for different TGAP-clay (2 wt% MMT) nanocomposites

Formulation	Impact energy/kJ m^{-2}	Standard deviation
TGAP/DDS	1.40	±0.18
TGAP/MMT/DDS, 150 ºC	1.60	±0.20
TGAP/MMT/DDS, 180 ºC	1.70	±0.38
TGAP/MMT/DDS, preconditioned at 40 ºC	2.10	±0.33
TGAP/MMT/DDS/BF_3 (0.5 wt%)	2.34	±0.24

Conclusions

Thermal analytical techniques, in particular but not exclusively Differential Scanning Calorimetry applied to the analysis of the cure kinetics, provide important information regarding the nanostructure development in epoxy-based polymer layered silicate nanocomposites. The ability to distinguish between the intra- and extra-gallery reactions allows the fabrication and cure procedures to be tailored in such a way as to optimise the resulting nanostructure. In this way it has been possible to progressively improve the

degree of exfoliation in epoxy nanocomposites, with a concomitant improvement in their mechanical properties. Thus thermal analysis can be seen to provide complementary information to that available from nanostructural characterisation techniques such as Small Angle X-ray Scattering and Transmission Electron Microscopy in respect of the ability or otherwise of the nanocomposite to attain a high degree of exfoliation.

Acknowledgements

This work was supported by MINECO project MAT2014-53706-C3-3-R. The authors are grateful to Huntsman Corporation for the TGAP epoxy resin and curing agent, and to Nanocor Inc. for the organically modified clay.

References

1. Kojima Y, Usuki A, Kawasumi M, Okada A, Kurauchi T, Kamigaito O. Synthesis of nylon-6-clay hybrid by montmorillonite intercalated with epsilon-caprolactam. J Polym Sci Part A, Polym Chem. 1993;31:983-986.

2. Usuki, A, Kawasumi M, Kojima Y, Okada A, Kurauchi T, Kamigaito, O. Swellinh behaviour of montmorillonite cation exchanged for omega-amino acids by epsilon-caprolactam. J Mater Res. 1993;8:1174-1178.

3. Usuki A, Kojima Y, Kawasumi M, Okada A, Fukushima Y, Kurauchi T, Kamigaito O. Synthesis of nylon 6-clay hybrid. J Mater Res. 1993;8:1179-1184.

4. Kojima Y, Usuki A, Kawasumi M, Okada A, Fukushima Y, Kurauchi T, Kamigaito O. Mechanical properties of nylon 6-clay hybrid. J Mater Res. 1993;8:1185-1189.

5. Azeez AA, Rhee KY, Park SJ, Hui D. Epoxy clay nanocomposites - processing, properties and applications: A review. Composites Part B – Engineering. 2013;45:308-320.

6. Hussain F, Hojjati M, Okamoto M, Gorga RE. Review article: Polymer-matrix nanocomposites, processing, manufacturing, and application: An overview. J Comp Mater. 2006;40:1511-1575.

7. Alexandre M, Dubois P. Polymer-layered silicate nanocomposites: preparation, properties and uses of a new class of materials. Mater Sci Eng. 2000;28:1-63.

8. Ray SS, Okamoto M. Polymer/layered silicate nanocomposites: a review from preparation to processing. Prog Polym Sci. 2003;28:1539-1641.

9. Becker O, Simon GP. Epoxy layered silicate nanocomposites. Adv Polym Sci. 2005;179:29-82.

10. Karak N. Polymer (epoxy) clay nanocomposites. J Polym Mater, 2006;23:1-20.

11. Liu WP. Epoxy-clay nanocomposites for structural applications. PhD Thesis, Concordia University, Quebec, Canada, 2005.

12. Lu JK, Ke YC, Qi ZN, Yi XS. Study on intercalation and exfoliation behavior of organoclays in epoxy resin. J Poly Sci Part B, Polym Phys. 2001;39:115-120.

13. Ton-That MT, Ngo TD, Ding P, Fang G, Cole KC, Hoa SV. Epoxy nanocomposites: Analysis and kinetics of cure. Polym Eng Sci. 2004;44:1132-1141.

14. Chen B, Liu J, Chen HB, Wu JS. Synthesis of disordered and highly exfoliated epoxy/clay nanocomposites using organoclay with catalytic function via acetone-clay slurry method. Chem Mater. 2004;16:4864-4866.

15. Miyagawa H, Rich MJ; Drzal, LT. Amine-cured epoxy/clay nanocomposites. I. Processing and chemical characterization. J Poly Sci Part B, Polym Phys. 2004;42:4384-4390.

16. Wang K, Chen L, Wu JS, Toh ML, He CB, Yee AF. Epoxy nanocomposites with highly exfoliated clay: Mechanical properties and fracture mechanisms. Macromolecules. 2005;38:788-800.

17. Liu WP, Hoa SV, Pugh M. Organoclay-modified high performance epoxy nanocomposites. Comp Sci Technol. 2005;65:307-316.

18. Hutchinson JM, Montserrat S, Román F, Cortés P, Campos L. Intercalation of epoxy resin in organically modified montmorillonite. J Appl Polym Sci. 2006;102:3751-3763.

19. Montserrat S, Cortés P, Pappin AJ, Quah KH, Hutchinson JM. Structural relaxation in fully cured epoxy resins. J Non-Cryst Sol. 1994;172-174:1017-1022.

20. Cortés P, Montserrat S, Hutchinson JM. Addition of a reactive diluents to a catalyzed epoxy-anhydride system. II. Effect on enthalpy relaxation. J Appl Polym Sci. 1997;63:17-25.

21. Calventus Y, Montserrat S, Hutchinson JM. Enthalpy relaxation of non-stoichiometric epoxy-amine resins. Polymer 2001;42:7081-7093.

22. Hutchinson JM. Studying the glass transition temperature by DSC and TMDSC. J Therm Anal Calorim. 2003;72:619-629.

23. Kamal MR. Thermoset characterization for moldability analysis. Polym Eng Sci. 1974;14:231-239.

24. Román F, Montserrat S, Hutchinson JM. On the effect of montmorillonite in the curing reaction of epoxy nanocomposites. J Therm Anal Calorim. 2007;87:113-118.

25. Montserrat S, Román F, Hutchinson JM, Campos L. Analysis of the cure of epoxy based layered silicate nanocomposites: Reaction kinetics and nanostructure development. J Appl Polym Sci. 2008;108:923-938.

26. Malek J. The kinetic analysis of non-isothermal data. Thermochim Acta 1992;200:257-269.

27. Benson Tolle T, Anderson DP. The role of preconditioning on morphology development in layered silicate thermoset nanocomposites. J Appl Polym Sci. 2004;91:89-100.

28. Pustkova P, Hutchinson JM, Román F, Montserrat S. Homopolymerization effects in polymer layered silicate nanocomposites based upon epoxy resin: Implications for exfoliation. J Appl Polym Sci. 2009;114:1040-1047.

29. Cortés P, Fraga I, Calventus Y, Román F, Hutchinson JM, Ferrando F. A new epoxy-based layered silicate nanocomposite using a hyperbranched polymer: Study of the curing reaction and nanostructure development. Materials 2014;7:1830-1849.

30. Shiravand F, Fraga I, Cortés P, Calventus Y, Hutchinson JM. Thermal analysis of polymer layered silicate nanocomposites: Identification of nanostructure development by DSC. J Therm Anal Calorim. 2014;118:723-729.

31. Varley RJ, Hodgkin JH, Hawthorne DG, Simon GP. Toughening of a trifunctional epoxy system. 2. Thermal characterization of epoxy/amine cure. J Appl Polym Sci. 1996;60:2251-2263.

32. Hutchinson JM, Shiravand F, Calventus Y, Fraga I. Isothermal and non-isothermal cure of a tri-functional epoxy resin (TGAP): A stochastic DSC study. Thermochim Acta 2012;529:14-21.

33. Hutchinson JM, Shiravand F, Calventus Y. Intra- and extra-gallery reactions in tri-functional epoxy polymer layered silicate nanocomposites. J Appl Polym Sci. 2013;128:2961-2970.

34. Shiravand F, Hutchinson JM, Calventus Y. Influence of the isothermal cure temperature on the nanostructure and thermal properties of an epoxy layered silicate nanocomposite. Polym Eng Sci. 2014;54:51-58.

35. Smith RE, Larsen FN, Long CL. Epoxy-resin cure. 2. FTIR analysis. J Appl Polym Sci. 1984;29:3713-3726.

36. Tackie M, Martin GC. The polymerization mechanism and kinetics of DGEBA with BF3-MEA. . J Appl Polym Sci. 1993;48:793-808.

37. Matejka L, Chabanne P, Tighzert L, Pascault JP. Cationic polymerization of diglycidyl ether of bisphenol-A. J Polym Sci Part A, Polym Chem. 1994;32:1447-1458.

38. Hutchinson JM, Shiravand F, Calventus Y, Fernandez-Francos X, Ramis X. Highly exfoliated nanostructure in trifunctional epoxy/clay nanocomposites using boron trifluoride as initiator. J Appl Polym Sci. 2014;131:Art. No. 40020(10pp).

39. Shiravand F, Hutchinson JM, Calventus Y, Ferrando F. Comparison of the nanostructure and mechanical performance of highly exfoliated epoxy-clay nanocomposites prepared by three different protocols. Materials 2014;7:4196-4223.

40. Hutchinson JM, Shiravand F, Calventus Y, Ferrando F. Comparative results between three protocols for achieving highly exfoliated epoxy-clay nanocomposites. Polimery 2014;59:636-642.